International Journal of Mechanical, Industrial and Aerospace Sciences
ISSN: 2517-9950
Vol:7, No:6, 2013

Laminar Free Convection of Nanofluid Flow in Horizontal Porous Annulus

Manal H. Saleh

***Abstract*—**A numerical study has been carried out to investigate the heat transfer by natural convection of nanofluid taking Cu as nanoparticles and the water as based fluid in a three dimensional annulus enclosure filled with porous media (silica sand) between two horizontal concentric cylinders with 12 annular fins of 2.4mm thickness attached to the inner cylinder under steady state conditions. The governing equations which used are continuity, momentum and energy equations under an assumptions used Darcy law and Boussinesq's approximation which are transformed to dimensionless equations. The finite difference approach is used to obtain all the computational results using the MATLAB-7. The parameters affected on the system are modified Rayleigh number ($10 \leq Ra^* \leq 1000$), fin length H_f (3, 7 and 11mm), radius ratio Rr (0.293, 0.365 and 0.435) and the volume fraction $(0 \leq \varphi \leq 0.35)$. It was found that the average Nusselt number depends on (Ra^*, H_f, Rr and φ). The results show that, increasing of fin length decreases the heat transfer rate and for low values of Ra^*, decreasing Rr cause to decrease Nu while for Ra^* greater than 100, decreasing Rr cause to increase Nu and adding Cu nanoparticles with 0.35 volume fraction cause 27.9% enhancement in heat transfer. A correlation for Nu in terms of Ra^*, H_f and φ, has been developed for inner hot cylinder.

***Keywords*—**Annular fins, laminar free convection, nanofluid, porous media, three dimensions horizontal annulus.

I. Introduction

MANY engineering applications are concerned with the natural convective flow in porous media in the recent years due to its wide applications in engineering such as solar collectors, drying processes, heat exchangers, geothermal and oil recovery, building construction, etc. A wide range of applications of porous media in practical problems can be found in the books [1]-[3]. A boundary layer analysis is presented for the natural convection heat transfer past a vertical flat plate embedded in a porous medium filled with nanofluids by [4] and past along two different geometries i.e., a vertical cone and an isothermal sphere in a Non-Darcy porous medium saturated with a nanofluid by [5]. Steady fully developed mixed convection flow of a nanofluid in a channel filled with a porous medium is presented by [6]. Steady mixed convection boundary layer flow from an isothermal horizontal circular cylinder embedded in a porous medium filled with a nanofluid has been studied for both cases of a heated and cooled cylinder by [7]. Laminar conjugate heat transfer by natural convection and conduction in a vertical annulus formed between an inner heat generating solid circular cylinder and an outer isothermal cylindrical boundary has been studied by a numerical method [8]. The governing equations have been solved using the finite volume approach, using SIMPLE algorithm on the collocated arrangement. Results are presented for Rayleigh number ranging from 10^5 to 10^8, solid volume fraction of $0<\varphi<0.05$ with copper-water nanofluid as the working medium. Considering that the driven flow in the annular tube is strongly influenced by orientation of tube, study has been carried out for different inclination angles. [9] Study numerically the effects of Grashof number and volume fraction of Cu-water nanofluid on natural convection heat transfer and fluid flow inside a two-dimensional wavy enclosure. Finite-Volume numerical procedure is used to solve the governing differential equations. Calculation were performed for the Grashof numbers from 10^4 to 10^6, nanoparticles volume fraction from 0% to 10% and surface waviness ranging from 0.0 to 0.4 for different patterns of wavy enclosure.

The schematic drawing of the geometry and the Cartesian coordinate system employed in solving the problem is shown in Fig. 1.

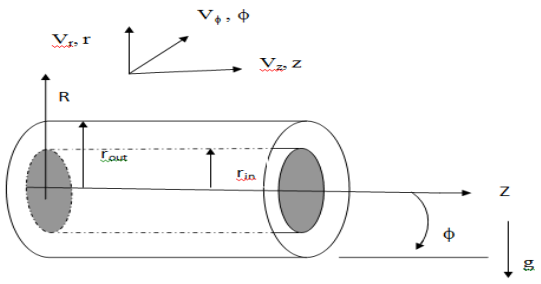

Fig. 1 Geometry and coordinate system

II. Mathematical Model

The effective thermal conductivity of the nano-fluid is approximated by Maxwell-Garnetts model:

$$\frac{k_{nf}}{k_f} = \frac{k_s + 2k_f - 2\phi\left(k_f - k_s\right)}{k_s + 2k_f + \phi\left(k_f - k_s\right)} \quad (1)$$

The use of this equation is restricted to spherical nano-particles where it does not account for other shapes of nano-particles. This model is found to be appropriate for studying heat transfer enhancement using nanofluid [7, 8]. The viscosity of the nanofluid can be approximated as viscosity of

Manal Hadi Saleh is Asst. Prof. at the Faculty in Mech. Dept./ College of Engineering/University of Baghdad (phone: 009647705833374, e-mail: manalhadi2005@yahoo.com).

a base fluid μ_f containing dilute suspension of fine spherical particles and is given by [9]:

$$\mu_{nf} = \frac{\mu_f}{(1-\phi)^{2.5}} \tag{2}$$

The governing equations (which used are continuity, momentum and energy equations) are transformed to dimensionless equations and the vector potential equation was obtained in the dimensionless form as [10] and [11]:

$$\frac{\partial U_r}{\partial R} + \frac{U_r}{R} + \frac{1}{R}\frac{\partial U_\phi}{\partial \phi} + \frac{\partial U_z}{\partial Z} = 0 \tag{3}$$

$$Ra^* \Pr * C_1 * \left(\sin\phi \frac{\partial \theta}{\partial Z}\right) = -\frac{\partial^2 \psi_r}{\partial R^2} - \frac{1}{R^2}\frac{\partial (R\psi_r)}{\partial R} - \frac{2}{R}\frac{\partial \psi_r}{\partial R} - \frac{1}{R^2}\frac{\partial^2 \psi_r}{\partial \phi^2} - \frac{\partial^2 \psi_r}{\partial Z^2} - \frac{2}{R}\frac{\partial \psi_z}{\partial Z} \tag{4}$$

$$Ra^* \Pr C_1 * \left(\cos\varphi \frac{\partial \theta}{\partial Z}\right) = -\frac{\partial^2 \psi_\phi}{\partial Z^2} - \frac{\partial^2 \psi_\phi}{\partial R^2} - \frac{1}{R^2}\frac{\partial^2 \psi_\phi}{\partial \phi^2} - \frac{2}{R^2}\frac{\partial \psi_r}{\partial \phi} + \frac{\psi_\phi}{R^2} - \frac{1}{R}\frac{\partial \psi_\phi}{\partial R} \tag{5}$$

$$-\frac{Ra^* \Pr C_1}{\alpha_{nf}}\left(\frac{1}{R}\cos\phi\frac{\partial\theta}{\partial\phi} + \sin\phi\frac{\partial\theta}{\partial R}\right) = -\frac{\partial^2 \psi_z}{\partial R^2} - \frac{1}{R}\frac{\partial \psi_z}{\partial R} - \frac{1}{R^2}\frac{\partial^2 \psi_z}{\partial \phi^2} - \frac{\partial^2 \psi_z}{\partial Z^2} \tag{6}$$

where $C_1 = \frac{\alpha_f}{\alpha_{nf}}\left[(1-\varphi) + \varphi\frac{(\rho\beta)_s}{(\rho\beta)_f}\right](1-\varphi)^{2.5}$

and the energy equation will be:

$$\left(\frac{1}{R}\frac{\partial\psi_z}{\partial\phi} - \frac{\partial\psi_\phi}{\partial Z}\right)\frac{\partial\theta}{\partial R} + \frac{1}{R}\left(\frac{\partial\psi_r}{\partial Z} - \frac{\partial\psi_z}{\partial R}\right)\frac{\partial\theta}{\partial\phi} + \left(\frac{\psi_\phi}{R} + \frac{\partial\psi_\phi}{\partial R} - \frac{1}{R}\frac{\partial\psi_r}{\partial\phi}\right)\frac{\partial\theta}{\partial Z} = \frac{\alpha_{nf}}{r_2}\left[\frac{\partial^2\theta}{\partial R^2} + \frac{1}{R}\frac{\partial\theta}{\partial R} + \frac{1}{R^2}\frac{\partial^2\theta}{\partial\phi^2} + \frac{\partial^2\theta}{\partial Z^2}\right] \tag{7}$$

and fin equation will be [12]:

$$\frac{\partial\theta}{\partial R} + \frac{\theta}{R} + \frac{1}{R}\frac{\partial\theta}{\partial\phi} + \frac{\partial\theta}{\partial Z} = 0 \tag{8}$$

For the vector potential field, the boundary conditions are given in Fig. 2.

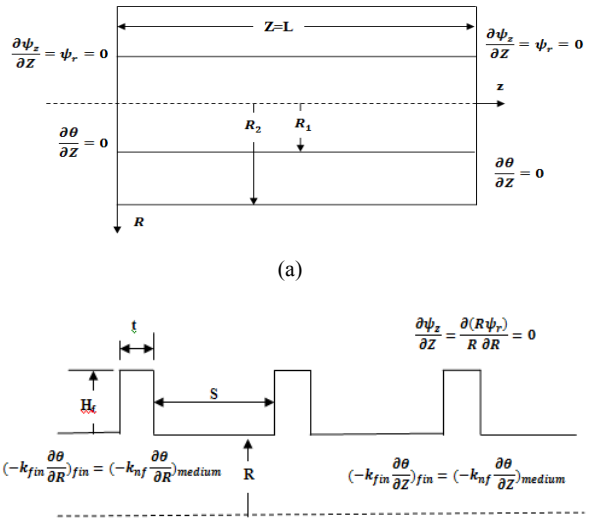

Fig. 2 (a) Annulus boundary conditions (b) Fins boundary conditions

III. Computational Technique

The equations were transformed into the finite difference approximation, where the upwind differential method in the left hand side of the energy equation and the centered – space differential method for the other terms were used, and solved by using (SOR) method [10]. A computer program was built using mat lab to meet the requirements of the problem. The value of the vector potential ψ calculated at each node, in which the value of vector potential is unknown, the other node will appear in the right hand side of each equation. The number of grid points used was 21 grid points in the R – direction, 31 in the ϕ – direction and 301 in the Z – direction.

IV. Calculation of Average Nusselt Number

The average Nusselt number Nu_{in} and Nu_{out} on the inner and the outer cylinders are defined as:

$$Nu_{in} = -(1-R_1)\frac{k_{nf}}{k_f}\frac{1}{\pi L}\int_0^L\int_0^\pi\left(\frac{\partial\theta}{\partial R}\right)_{R=R} d\phi\, dZ \tag{9}$$

$$Nu_{out} = -(1-R_1)\frac{k_{nf}}{k_f}\frac{1}{\pi L}\int_0^L\int_0^\pi\left(\frac{\partial\theta}{\partial R}\right)_{R=1} d\phi\, dZ \tag{10}$$

V. Results and Discussion

A. Temperature and Streamlines Field

The dimensionless temperature distribution within the enclosure is presented in a contour map form. One section was selected in the (Z-R) plane along the length of the annulus, and the other in the (R-ϕ) plane, in a manner allowed studying the temperature distribution and streamlines within each plane.

Fig. 3 shows the temperature distribution for horizontal annulus and it was observed that for pure fluid (volume fraction φ=0), isotherms shift towards the outer (cold) cylinder where the waviness in temperature distribution is due to the existence of the fins, and a high temperature exist in the upper half of the annulus while a thicker cold layer in the lower region of the annulus wall exist.

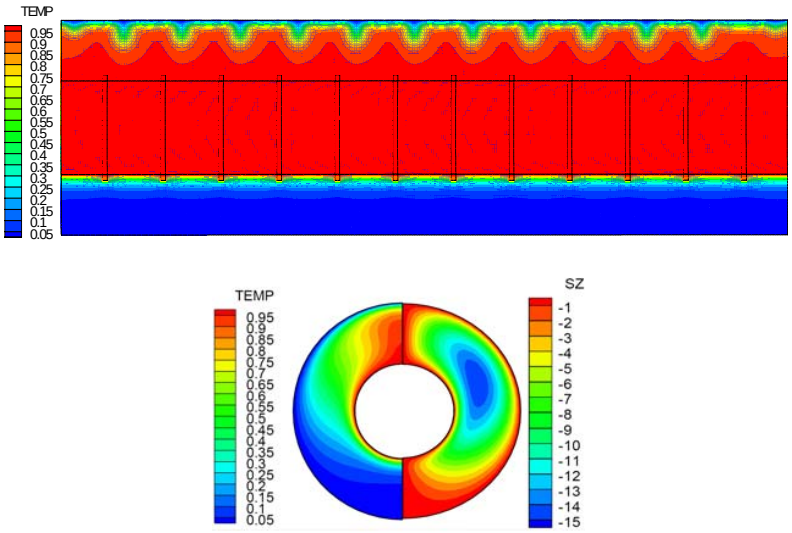

Fig. 3 Isotherm and streamlines for Hf=3
Ra=1000, φ=0, Rr=0.435

The fluid rises after being heated on the inner cylinder surface, then impinges on to the top of outer cylinder surface where it is cooled and flows down along the outer circumference. Far away from the inner cylinder, the isothermal lines are deformed from their conductive pattern, and become curvilinear indicating that an ascending and descending convective flows occur. The streamlines illustrate the contour as unicellular of negative value at center and positive at the boundaries.

Adding nanoparticles cause to enhance heat transfer as shown in Fig. 4 where it is clear that the temperature decrease and the isothermal lines in the upper region of the cylinder abate and come close to the wall, while the cold region in the lower half of the cylinder widens. Fig. 5 shows the effect of fin length for pure fluid for the same values of Ra and Rr as in Fig. 3. It is clear that increasing Hf cause to decrease the heat transfer and the streamlines have greater values at the lower cold region and the cellular retreat directed toward the upper region.

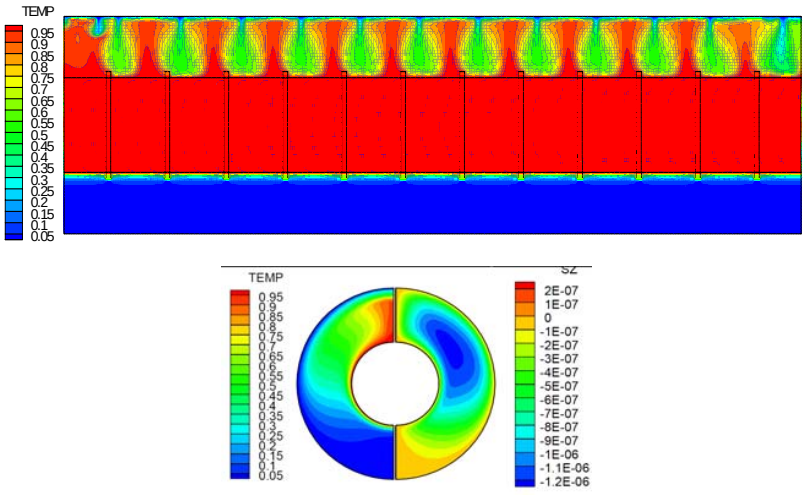

Fig. 4 Isotherm and streamlines for Hf=3
Ra=1000, φ=0.35, Rr=0.435

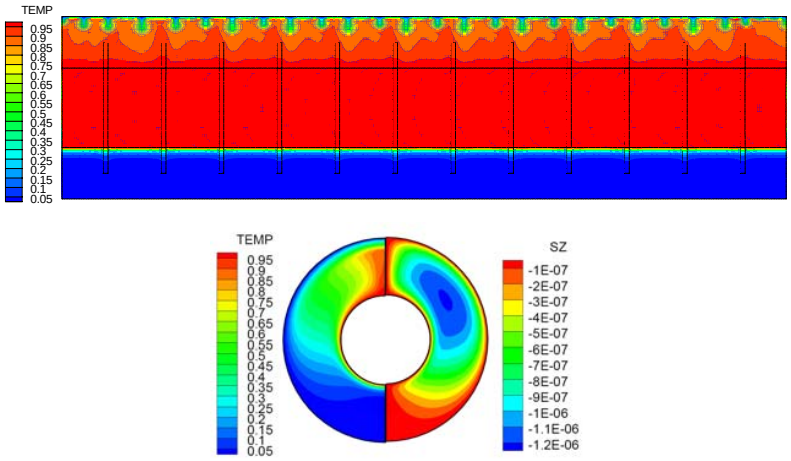

Fig. 5 Isotherm and streamlines for Hf=11
Ra=1000, φ=0, Rr=0.435

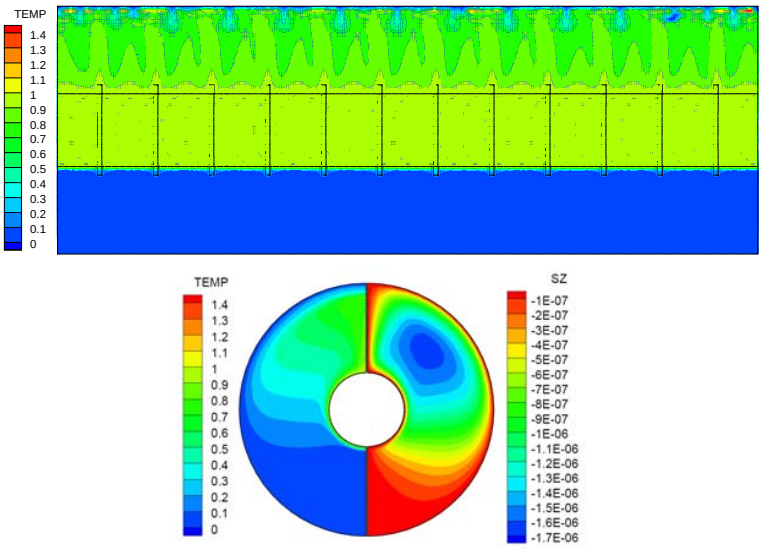

Fig. 6 Isotherm and streamlines for Hf=3
Ra=1000, φ=0.35, Rr=0.293

Decreasing the radius ratio which means increasing the gap between the cylinders for φ=0.35 as shown in Fig. 6 illustrates that the region will be cold and a definite enhancement in heat transfer will be occur.

A swell of the isothermal lines can observed when Ra^* increase which implies to the increase in Nu. Decreasing the radius ratio Rr means increasing the gap between the cylinders which cause a decrease in temperature much faster.

B. Velocity Fields, Vector Potential

Fig. 7 illustrates high values of the velocity on the two faces of the fins and on the tip causing the fluid to rise up toward the outer cylinder and adding Cu particles cause enhancement in heat transfer and increase of velocity in the upper half of the annulus will be clearly while the lower region of the annulus cooled and the velocity of the fluid reduced.

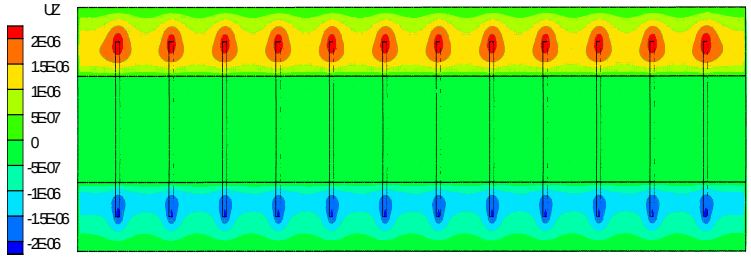

Hf=11, Ra*=100, φ =0

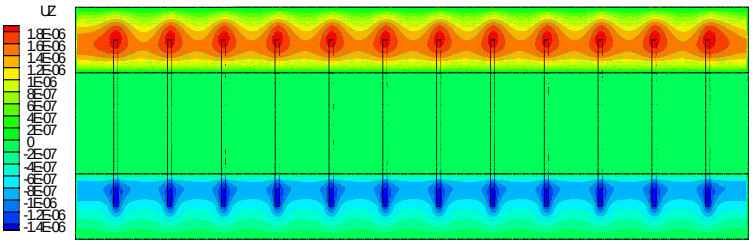

Hf=11, Ra*=100, φ =0.35

Fig. 7 Variation of Uz for different values of Hf, Ra* and φ

C. Effect of Modified Rayleigh Number and Other Parameters

Fig. 8 shows the variation of the average Nusselt number on the cylinders with *Ra** for different radius ratios. These figures show that for any radius ratio, the average *Nu* generally constant for low values of Ra* then as Ra* reached nearly 100, *Nu* increased with increasing *Ra**. These values increased as *Rr* decrease due to the enlarge of the gap between the two cylinders.

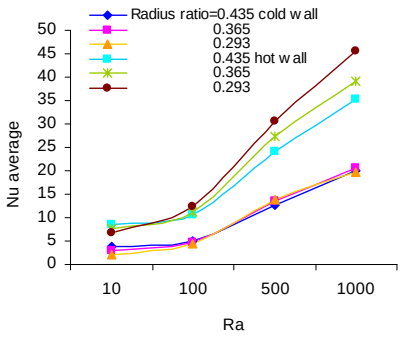

Fig. 8 Variation of average Nu with Ra for different radius ratio

Fig. 9 indicates that there is a reduction in the average Nusselt number with increasing H_f from 3mm to 11mm. For the same value of Ra*, reduction in the average Nusselt number ranged between (18% to 38 %).

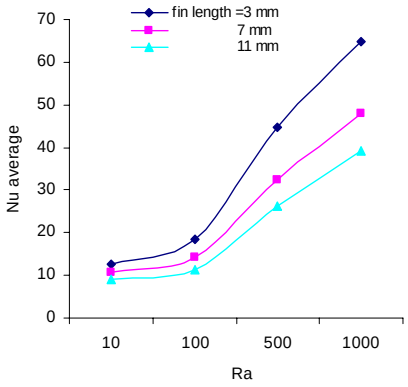

Fig. 9 Variation of average Nu with Ra for different fin length

A correlation for Nu in terms of Ra, H_f and φ, has been developed for inner hot cylinder as follow:

$$Nu = 16.045 \frac{Ra^{0.282}\varphi^{0,552}}{H_f^{0.353}} \quad (11)$$

Fig. 10 presents the variation of average Nusselt number with modified Rayleigh number for different values of volume fraction. The figure shows that the heat transfer increases almost monotonically with increasing the volume fraction for all Ra*. As volume fraction of nanoparticles increases, difference for average Nusselt number becomes larger especially at higher Ra* due to increasing of domination of convection mode of heat transfer. Effect of nanoparticles on

enhancement of heat transfer at high Ra^* is more significant than that at low Ra^*.

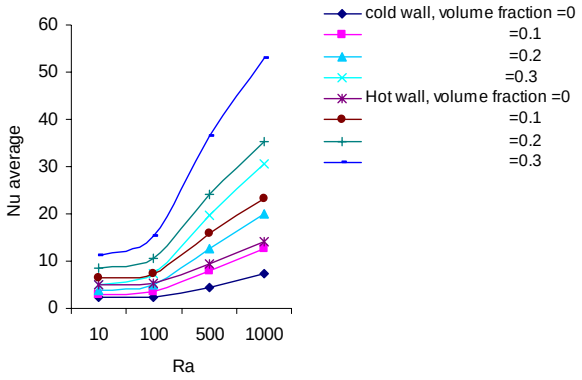

Fig. 10 Variation of average Nu with Ra for different volume fraction

Fig. 11 shows the variation of average Nusselt number with volume fraction for different values fin length. The figure illustrates that Nusselt number increases with the volume fraction and for Ra^* =1000 and φ =0.35 the reduction in average Nusselt number is 65.5% when using fin of length Hf =11mm instead of Hf=3mm.

The variation of average Nusselt number with volume fraction for different values of radius ratio Rr is shown in Fig. 12. It is clear that as Rr decrease which means increasing the gap between the cylinders, Nusselt number increases because the convection heat transfer is the dominant mode. For volume fraction φ =0.35 and Ra^* =500, the reduction in average Nusselt number is 27.93% between Rr= 0.435 and 0.293.

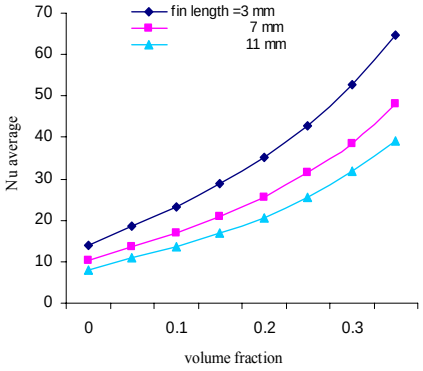

Fig. 11 Variation of average Nu with volume fraction for different fin length

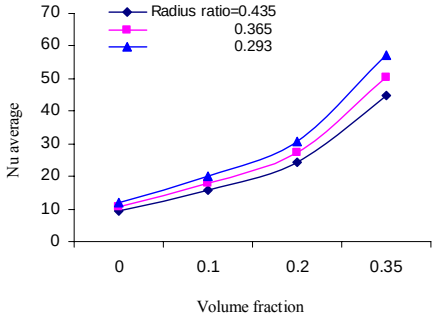

Fig. 12 Variation of average Nu with volume fraction for different radius ratio

VI. Conclusions

The following major conclusions can be drawn from the experimental and numerical study:

Average Nu number increases with increasing fin length at the same Ra^* and fin number unless the surface area of the inner cylinder exceeds that of the outer cylinder, then the heat will be stored in the porous media. Maximum value of local Nu number increasing with the increase of inclination angle and it may be reached twice the value of that for horizontal cylinder. For all parameters, results showed that the average Nu number increases with an increase in modified Rayleigh number and hardly affected by δ for low values of Ra^*. Increasing Rr cause a clearly increase in average Nusselt number for Ra^*› 100.

The peak of the local Nu on the outer cylinder wall generally appeared at a position of Z=L (at the top) and ϕ with some deviation from π. while for the inner cylinder the peak appeared at a position of Z=0 (bottom of the cylinder).

TABLE I
Nomenclature

Symbol	Description	Unit
C_p	magnetic flux	kJ/kg °C
g	Acceleration due to	m/s^2
H_f	Fin length	m
k_f	Thermal conductivity of the fluid	W/m K
K_{nf}	Thermal conductivity of nanofluid	W/m K
k_s	Thermal conductivity of solid (nanoparticles)	W/m K
L	Dimensionless cylinder length	-
p	Pressure	N/m^2
Pr	Prandtl number	-
R	Dimensionless radial coordinate	m
S	Fin pitch	m
U_r, $U_□$, U_z	Dimensionless velocity component in R, ϕ and Z direction	-
Z	Dimensionless axial coordinate	-
θ	Dimensionless temperature	-
φ	Volume fraction	-
μ_f	Dynamic viscosity of fluid	Pa.s
μ_{nf}	Dynamic viscosity of nanofluid	Pa.s
α_f	Fluid thermal diffusivity	m^2/s
α_{nf}	Nanofluid thermal diffusivity	m^2/s
ψ_r, $\psi_□$, ψ_z	Vector potential component in R, ϕ and Z – direction	-

REFERENCES

[1] D.A. Nield, A. Bejan, Convection in Porous Media, third ed., Springer, New York, 2006.
[2] D. Ingham, I. Pop, Transport Phenomena in Porous Media, vol. III, Elsevier, Oxford, 2005.
[3] I. Pop, D.B. Ingham, Convective Heat Transfer: Mathematical and Computational Modeling of Viscous Fluids and Porous Media, Pergamon, Oxford, 2001.
[4] Syakila Ahmad, Ioan Pop, Mixed convection boundary layer flow from a vertical flat plate embedded in a porous medium filled with nanofluids, International communication in Heat and Mass transfer 37 (2010) 987-991.
[5] Kaustubh Ghodeswar, Natural Convection in a Porous Medium Saturated by Nanofluid, M.Sc. thesis, Cleveland State University, December, 2010.
[6] Dalia Sabina Cimpean, Ioan Pop, Fully developed mixed convection flow of a nanofluid through an inclined channel filled with a porous medium, International communication in Heat and Mass transfer 55 (2012) 907-914.
[7] R. Nazar · L. Tham · I. Pop · D. B. Ingham, Mixed Convection Boundary Layer Flow from a Horizontal Circular Cylinder Embedded in a Porous Medium Filled with a Nanofluid, Transp Porous Med (2011) 86:517–536
[8] Mina Shahi, Amir Houshang Mahmoudi, Farhad Talebi, A numerical investigation of conjugated-natural convection heat transfer enhancement of a nanofluid in an annular tube driven by inner heat generating solid cylinder, International communication in Heat and Mass transfer 38 (2011) 533-542
[9] M. Esmaeilpour, M. Abdollahzadeh, Free convection and entropy generation of nanofluid inside an enclosure with different patterns of vertical wavy walls, International Journal of Thermal Science 52 (2012)127-136
[10] Wang Bu – Xuan and Zhang Xing, "Natural Convection in Liquid Saturated Porous Media Between Concentric Inclined Cylinders" Int. J. Heat and Mass Transfer Vol. 33. No 5, pp. 827-833, 1990.
[11] Fukuda K., Takata Y., Hasegawa S., Shimomura H. and Sanokawa K., "Three – Dimensional Natural Convection in a Porous Medium Between Concentric Inclined Cylinders", Proc. 19th Natl Heat Transfer Conf., Vol. HTD – 8, pp. 97 – 103, 1980
[12] Ramón L. F. and Sergio G. M., "Three Dimensional Natural Convection in Finned Cubical Enclosure", Int. J. of Heat and Fluid Flow, Vol. 28, pp. 289 – 298, 2007.